Advances in Aircraft and Spacecraft Science, *Vol. 9, No. 4 (2022) 279-300*
https://doi.org/10.12989/aas.2022.9.4.279

An effective method for detecting satellite orbital maneuvers and its application to LEO satellites

Abdikul E. Ashurov*

Department of Space Engineering and Technology, L.N. Gumilyov Eurasian National University, 2 Satpayev, Nur-Sultan, 010008, Republic of Kazakhstan

(Received March 13, 2022, Revised May 25, 2022, Accepted June 7, 2022)

Abstract. This paper analyzes the possibilities of a new method to using TLE data for detecting satellite maneuvers. The method has a number of advantages over other methods that are designed to detect maneuvers. It allows not only to detect maneuvers, but also to get a more complete picture of the maneuver. In particular, the method makes it possible to estimate the moments of the beginning and end of the maneuver, calculate the changes in the orbital elements, evaluate the tangential and binormal components of the impulse, and finally, calculate the impulse of the satellite obtained as a result of the maneuver. To demonstrate in detail the capabilities of the algorithm, the proposed method was applied to one of LEO satellites - TIANHUI-1 satellite. After the efficiency of the method was proved, this method was applied to the China Space Station - TIANHE-1 (CSS), Starlink-1095 and Starlink-2305 satellites. The maneuvers of the CSS and Starlink-1095 satellite during their close encounter on 1 July, 2021, and the CSS and Starlink-2305 satellite during their close encounter on 21 October, 2021 are analyzed in detail. The minimum distances between the CSS and Starlink satellites at the moments of their maximum approaches are estimated. An estimate of the computation time of this algorithm is given, and the possibility of its use for monitoring maneuvers or other anomalous orbital changes of a large number of satellites in near real-time is shown. It is assumed that on the basis of this method, a service for monitoring satellite maneuvers can be created.

Keywords: China Space Station; LEO satellite; maneuver detection; satellite maneuver; Starlink satellite; two-line element

1. Introduction

In December 2021, China sent a Note to the UN claiming that it had to perform evasive maneuvers on its space station to avoid potential collisions with two SpaceX Starlink satellites (United Nations 2021). In the Note, China details the collision avoidance between the China Space Station (international designation 2021-035A) and United States' Starlink-1095 (international designation 2020-001BK) and Starlink-2305 (international designation 2021-024N) satellites. As stated in this document, between 16 May and 24 June 2021, the Starlink-1095 satellite maneuvered continuously to an orbit of around 382 km, and then stayed in that orbit. A close encounter occurred between the Starlink-1095 satellite and the China Space Station on 1 July 2021. For safety reasons, the China Space Station took the initiative to conduct an evasive maneuver in the evening of that day to avoid a potential collision between the two spacecraft. The second incident

*Corresponding author, Ph.D., E-mail: ashurov_ae@enu.kz

http://www.techno-press.org/?journal=aas&subpage=7 ISSN: 2287-528X (Print), 2287-5271 (Online)

occurred on October 21, 2021, when the Starlink-2305 satellite had a subsequent close encounter with the China Space Station. As the satellite was continuously maneuvering, the maneuver strategy was unknown and orbital errors were hard to be assessed, there was thus a collision risk between the Starlink-2305 satellite and the China Space Station. To ensure the safety and lives of in-orbit astronauts, the China Space Station performed an evasive maneuver again on the same day to avoid a potential collision between the two spacecraft.

Prior to this, in September 2019, the European Space Agency stated that September 2 the Aeolus satellite performed a maneuver to avoid a potential close approach to a Starlink satellite, which it identified in one graphic as Starlink 44 - one of the first 60 satellites launched in SpaceX's mega constellation (ESA 2019). According to a list of conjunctions called the Satellite Orbital Conjunction Reports Assessing Threatening Encounters in Space (SOCRATES), maintained by the Center for Space Standards & Innovation, Aeolus was predicted to have a close approach shortly after 7 a.m. Eastern September 2 with a satellite identified as "Starlink AV" for its international designation, 2019-029AV (Spacenews 2019), i.e., Starlink-67 satellite with NORAD ID 44278.

These two cases are examples of successful satellite maneuvering to avoid collision. But due to the rapid increase in satellites in orbit, the chances of satellite collisions are also increasing. In this situation, it is important not only to predict the probability of a collision in time and to carry out evasive maneuvers in time, but also to analyze the results of the maneuvers performed. This is necessary in order to evaluate the effectiveness of satellite control, develop a strategy for satellite control, notify users and operators of other satellites in a timely manner about changes in the orbit of this satellite, and recheck the probability of collision with this satellite again, and if necessary, take the necessary measures to reduce the probability of satellite collisions. In addition, the analysis of maneuvers will make it possible to estimate the consumption and remaining fuel of the spacecraft. Of course, in order to see changes in the orbit as a result of the maneuvers performed, it is enough to re-determine the orbit. But this does not give a complete picture of the maneuvers. In particular, in this way it is impossible to determine the magnitude of tangential and binormal impulses, using which changes in the semi-major axis, eccentricity and inclination of the orbit are made. For these purposes, methods that meet these requirements are needed. Based on this, we propose an efficient method for detecting performed maneuvers and determining the magnitude of impulses.

The detection of satellite maneuvers is one of the important tasks of space surveillance and space situation awareness. Despite the fact that over the past two decades, quite a lot of works have been devoted to this issue and effective methods for detecting maneuvers have been proposed, this problem has not yet been fully solved. As an overview on this topic, we can point to the work of Chen *et al*. (2017). And as one of the first methods of using two-line element (TLE) data to detect satellite maneuvers, one can point to Kelecy *et al*. (2007). Algorithm performance is measured relative to Topex (SSN# 22076) and Envisat (SSN# 27386) satellites with known maneuver histories. The results show reliable detection of maneuvers down to delta-velocity magnitudes at the centimeter-per-second level or less. Another data processing method for detecting space collisions and satellite maneuvers is developed by Patera (2008). The method uses state vector data associated with the catalog of tracked objects and it can be applied to any element set parameter or a derivative of one or more TLE parameters. The statistical distribution of the parameter dispersion is used to establish an event threshold. Maneuver is declared when dispersions exceed the event threshold.

Lemmens and Krag (2014) presented two methods of detecting a maneuver based on the

analysis of satellite two-line elements history. The first method called the TLE consistency check (TCC), is based on consistency checking between consecutive TLEs and the comparison of this consistency with a reference population. Another method, called TLE time series analysis (TTSA), can avoid some theoretical drawbacks of earlier methods from the same category. The performances of these methods are verified on detected maneuvers performed in 2011 by LEO meteorological satellites. Another maneuver detection method based on historical two-line element (TLE) data for low Earth orbit satellites is described in Li *et al*. (2018). The historical maneuvers of a satellite are detected by identifying abnormal data segments in the TLE derived time series of semi-major axis and inclination. When the anomaly index of a semi-major axis segment or inclination segment exceeds the corresponding threshold, a specific type of orbit maneuver with specific magnitude is declared. The maneuver detection results of Terra and METOP-A indicate that the proposed method provides reasonably reliable detection of satellite maneuvers.

Maneuver detection method based on probability distribution fitting of the prediction error described in Li *et al*. (2019). An analysis of the prediction error between the published state of a specific orbital parameter and the prediction state is used in the method. The threshold of detecting abnormal values of the orbital parameter is derived based on obtained probability distributions. To eliminate noise interference, a method of detecting historical orbital maneuvers from the TLE-derived semi-major axis sequence of the satellite is specially designed.

Bai *et al*. (2019) proposed a method where data clustering analysis is used to detect the orbital maneuvers of satellites. The authors use the unsupervised classification methods of K-means, hierarchical, and fuzzy C-means clustering to handle the two-line element data. Three levels of orbital maneuvers were identified using the above three methods. The method was applied to detect the maneuvers of the Yaogan-9, Tianhui-1 and Envisat satellites.

Since speed is important for real time space situational awareness (SSA), the throughput of maneuver detection algorithms needs to increase. With the goal of increasing the computational speed and accuracy of maneuver detection, Clark and Lee (2020) outlined approaches to increase the performance of SSA algorithms. Parallel processing is implemented in orbital maneuver detection methods by fusing TLE analysis and state propagation method into a hybrid detection method.

TLEs that play critical roles in space monitoring and analysis activities, suffer from uneven data quality and it is usually necessary to perform outlier or anomaly detections before utilizing these ephemerides. Liu *et al*. (2021) proposed a TLE outlier detection filter based on the Expectation Maximization algorithm. In this case the outlier thresholds are set based on the evaluated variances which are statistically determined in the polynomial regression and prediction and thus, there is no need to determine them manually.

Mukundan and Wang (2021) proposed simplified approach to detect satellite maneuvers based on TLE data and SGP model. In this study, an algorithm was set to detect sudden changes in the orbital parameters by calculating the difference between the adjacent segments of the orbital parameters propagated by SGP4 and the observed orbital parameters extracted directly from the TLEs. Five observed orbital parameters, comprising semi-major axis, inclination, right ascension of the ascending node, eccentricity, and orbital energy, were extracted. Thus, the difference between the Keplerian elements (the orbital parameters propagated by SGP4 through the state vectors) and non-Keplerian elements (five observed orbital parameters extracted directly from the TLEs) is used to detect maneuvers. Although here it would be appropriate to speak of osculating elements rather than Keplerian elements. Moreover, one TLE was chosen per day to study the orbital parameters. The method was applied to the TOPEX and Envisat satellites.

As the review of works devoted to the issue of detecting maneuvers of satellites shows, the most developing direction in the development of methods for detecting maneuvers is the use of historical TLE data of satellites. So taking into account the experience of other works, we propose to further develop a method that uses historical TLE data. Moreover, we propose to use the difference of two osculating elements, which are both obtained by propagation using the SGP4 model. As we see in Mukundan and Wang (2021), the difference between Keplerian and non-Keplerian (and non-osculating) orbital elements is used. In addition, it is necessary to use exclusively all TLE data, without selecting specific points. Because choosing some TLE data for calculation, and not using the rest of the data, will lead to the loss of information. Moreover, the developed method should give a more complete picture of the maneuver, in particular, information about the duration of the maneuver, the values of the tangential and binormal components of the impulse, and, accordingly, the value of the impulse ΔV itself.

The aim of the study is to examine a new, effective approach to using TLE data for detecting satellite maneuvers, as well as to calculating the value of the impulse obtained by the satellite from the maneuver. The organization of this paper is as follows: proposed algorithm for maneuver detection is described in Section 2, the maneuver detection results presented in Section 3, discussions and conclusions in Section 4.

2. Proposed maneuver detection and analysis algorithm

As noted in the Introduction we propose to use the difference of two osculating elements, which are both obtained by propagation using the SGP4 model. The SGP4 model is one of Simplified Perturbations models (SGP, SGP4, SDP4, SGP8 and SDP8) that are used to calculate orbital state vectors of satellites and space debris relative to the Earth-centered inertial coordinate system (Hoots and Roehrich, 1980). Simplified General Perturbations (SGP) models apply to near Earth objects with an orbital period of less than 225 minutes. Simplified Deep Space Perturbations (SDP) models apply to objects with an orbital period greater than 225 minutes, which corresponds to an altitude of 5877.5 km, assuming a circular orbit. SGP4 propagation algorithms consider the main perturbation influences on a satellite: first four zonal Earth gravity field harmonics, atmospheric drag and solar radiation pressure. SDP4 adds luni-solar gravity attraction and deep space secular effects. All these models use two-line element sets (TLE) as input data, produced by NORAD (North American Aerospace Defense Command) and NASA (National Aeronautics and Space Administration). The TLE are general perturbation mean elements constructed by a least squares estimation from observations of a satellite's orbit and by removing periodic variations in the force model due to the oblateness of the Earth, atmospheric drag, and lunar and solar gravitational effects. In order to obtain good predictions from the TLE, the periodic variations must be reconstructed in exactly the same way they were removed. We use the SGP4 model in our work.

The proposed algorithm consists of the following steps.

1. Reading and loading historical TLE data for a given satellite.
2. If two consecutive records refer to the same epoch, then to take only the last record.
3. For each epoch of TLE data, using the SGP4 model, determine the satellite state vector (coordinates x, y, z and velocity components v_x, v_y, v_z in the Earth-centered inertial coordinate frames).
4. From the state vector at each moment of the epoch t_k, determine the osculating elements and

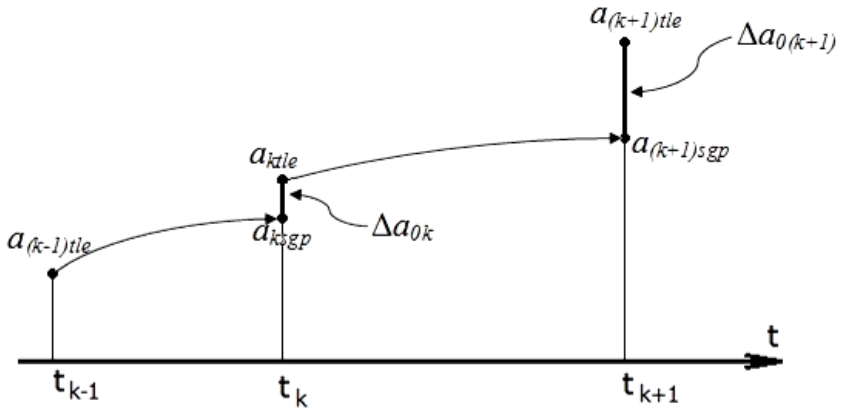

Fig. 1 Calculating Δa_{0k}

denote them, for example, as $(a, e, i, \Omega, \omega, f)_{\text{ktle}}$ (it is not simply extracting orbital parameters from TLE data).

5. Using the SGP4 propagator, from the TLE data of the t_{k-1} epoch, determine the satellite state vector to the t_k epoch, where $k=2,..., N$, and N is the number of TLE sets. This process is similar to "natural changes" in the parameters of the orbit, without any anomalies.

6. From the obtained state vector for t_k time moment, calculate the osculating elements and denote them, for example, as $(a, e, i, \Omega, \omega, f)_{\text{ksgp.}}$

7. For each time moment t_k, where $k=2,\ldots, N$, calculate the differences $\Delta a_{0k}=a_{ktle}-a_{ksgp}$ and $\Delta i_{0k}=i_{ktle}-i_{ksgp}$ (Fig. 1). Purely theoretically, without taking into account the errors in the TLE data, in the absence of any anomalous changes, this difference should be equal to zero. And its high value, on the contrary, will show anomalous changes in the parameters of the orbit.

8. Using the graphs $\Delta a_{0k}(t)$ and $\Delta i_{0k}(t)$ estimate thresholds for the semi-major axis a_{thr} and for the inclination i_{thr} ($a_{\text{thr}}>0$ and $i_{\text{thr}}>0$). Since the thresholds are, in fact, some kind of background noise, in the next step we remove all points that are below the noise level.

9. Discard the values $\Delta a_{0k}(t)$ and $\Delta i_{0k}(t)$ satisfying the conditions $|\Delta a_{0k}(t)|< a_{\text{thr}}$ and $|\Delta i_{0k}(t)|< i_{\text{thr.}}$

10. Using the remaining values of $\Delta a_{0k}(t)$ and $\Delta i_{0k}(t)$, calculate the values $\Delta a_k(t)$ and $\Delta i_k(t)$ taking into account the thresholds: as $\Delta a_k=\Delta a_{0k}-a_{\text{thr}}$ and $\Delta i_k=\Delta i_{0k}-i_{\text{thr}}$ for positive Δa_{0k} and Δi_{0k}, and as $\Delta a_k=\Delta a_{0k}+a_{\text{thr}}$ and $\Delta i_k=\Delta i_{0k}+i_{\text{thr}}$ for negative ones. Thus, we now have the filtered differences Δa_k и Δi_k.

11. Using Δa_k calculate the tangential component of the impulse $\Delta v_{ktan}=\Delta a_k \cdot v_k/(2a_{\text{ktle}})$ (Hu 2015), where $v_k=(v_x^2+v_y^2+v_z^2)^{1/2}$ is the satellite speed at the time epoch of t_k.

12. Using Δi_k calculate the binormal component of the impulse $\Delta v_{kbin}=2v_k \cdot \sin(\Delta i_k/2)$ (Curtis 2020).

13. Evaluate the satellite impulse as $\Delta v_k=(\Delta v_{ktan}^2+\Delta v_{kbin}^2)^{1/2}$.

3. Application to LEO satellites

To demonstrate in detail the algorithm and the capabilities of the method, we started the application of the proposed method with TIANHUI-1 satellite (NORAD ID 36985). After the efficiency of the method was proved by comparing our results with the results of other authors,

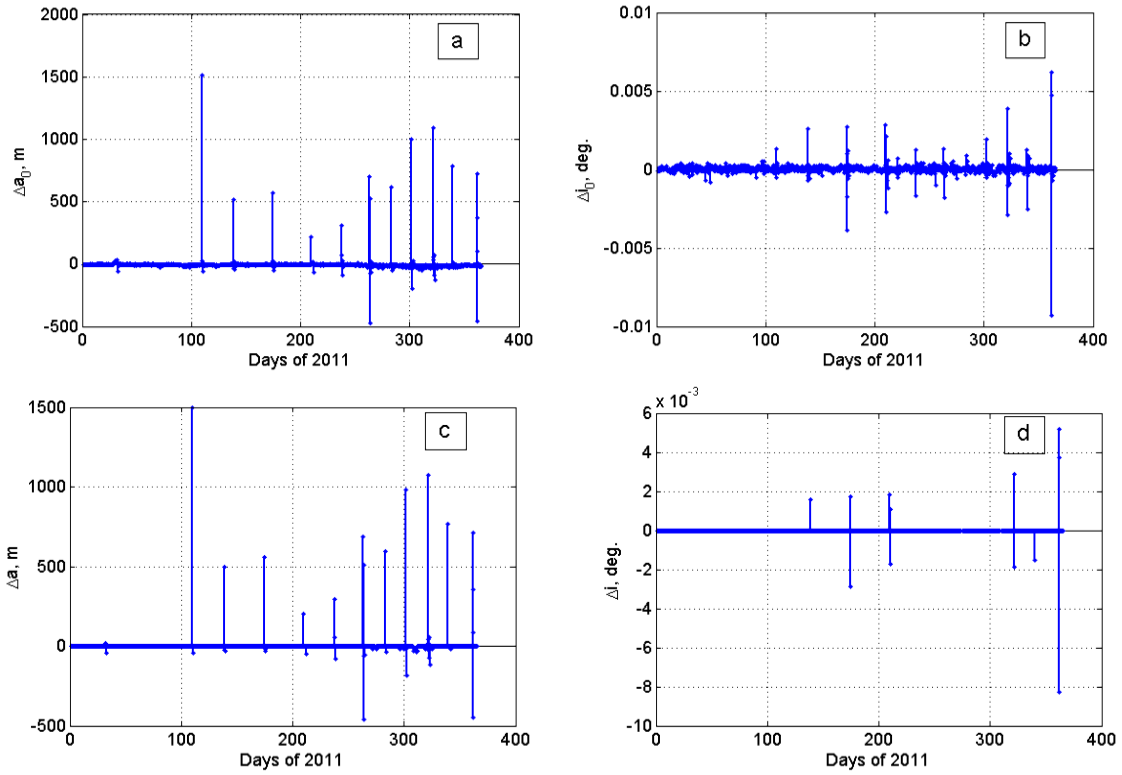

Fig. 2 Δa_0 (a) and Δi_0 (b) differences for the TIANHUI-1satellite without taking into account the thresholds, Δa_k (c) and Δi_k (d) differences with taking into account the thresholds of a_{thr}=15 m and i_{thr}=0.001 degree

this method was applied to the China Space Station - TIANHE-1 (NORAD ID 48274), Starlink-1095 (NORAD ID 44971) and Starlink-2305 (NORAD ID 47989) satellites. The historical TLEs for all satellites were downloaded from the CelesTrak website (2022).

3.1 TIANHUI-1

The TLEs of the TIANHUI-1 satellite between 2011-01-01 and 2011-12-31 are processed. Following steps 1 through 7 of the method described in Section 2, we found the $\Delta a_{0k}=a_{ktle}-a_{ksgp}$ and $\Delta i_{0k}=i_{ktle}-i_{ksgp}$ as differences between the observed semi-major axis and inclination obtained from the TLE data and those extrapolated from the previous moment using the SGP4 model. The corresponding diagrams of values $\Delta a_{0k}(t)$ and $\Delta i_{0k}(t)$ are shown in Fig. 2 (a) and (b).

On this graph positive values of the change in the semi-major axis and inclination correspond to an increase in these values. From these graphs, we estimated the thresholds on the semi-major axis as a_{thr}=15 m and on the inclination as i_{thr}=0.001 degree. And by performing steps 9 and 10, we calculate the values $\Delta a_k(t)$ and $\Delta i_k(t)$ taking into account the thresholds: as $\Delta a_k=\Delta a_{0k}-a_{\text{thr}}$ and $\Delta i_k=\Delta i_{0k}-i_{\text{thr}}$ for positive Δa_{0k} and Δi_{0k}, and as $\Delta a_k=\Delta a_{0k}+a_{\text{thr}}$ and $\Delta i_k=\Delta i_{0k}+i_{\text{thr}}$ for negative ones. Since the thresholds are, in fact, some kind of background noise, in step 9 we remove all points that are below the noise level, i.e., discard the values $\Delta a_{0k}(t)$ and $\Delta i_{0k}(t)$ satisfying the conditions $|\Delta a_{0k}(t)|<a_{\text{thr}}$ and $|\Delta i_{0k}(t)|< i_{\text{thr}}$. The results obtained are presented in Fig. 2 (c) and (d).

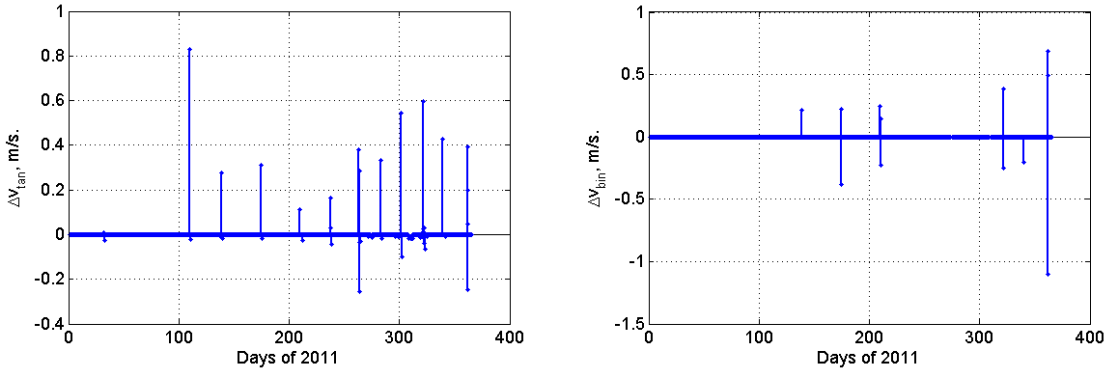

Fig. 3 Tangential and binormal components of the TIANHUI-1 maneuver impulses

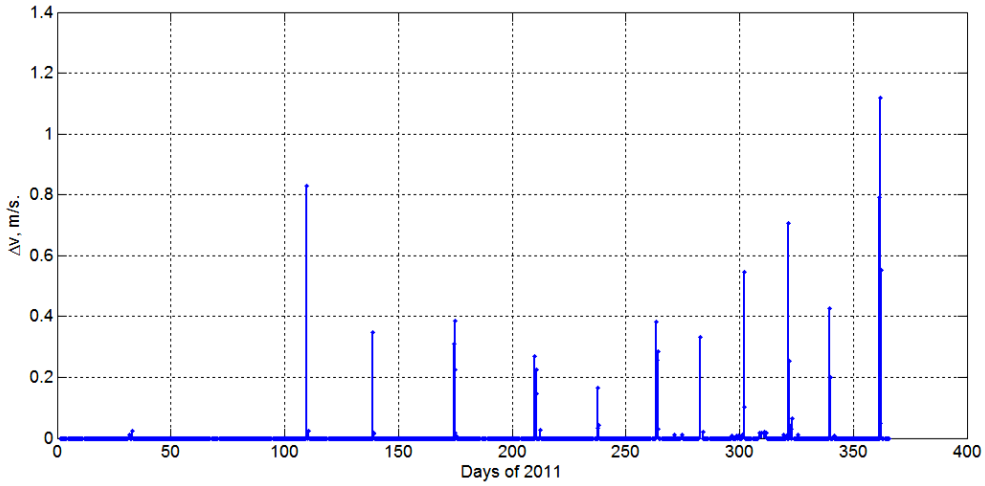

Fig. 4 Maneuver impulses determined from tangential and binormal components for TIANHUI-1

Further, according to steps 11 and 12 of our algorithm, the tangential components of the impulse Δv_{ktan} and the binormal ones Δv_{kbin} are calculated from the filtered values of Δa_k and Δi_k. The results are shown in Fig. 3. In this case, we assumed that the orbit is almost circular and e≈0. Therefore the tangential component is calculated as $\Delta v_{ktan}=\Delta a_k \cdot v_k/(2a_{ktle})$ (Hu 2015), where $v_k=(v_x^2+v_y^2+v_z^2)^{1/2}$ is the satellite speed at the time epoch of t_k; and the binormal component is calculated as $\Delta v_{kbin}=2v_k \cdot \sin(\Delta i_k/2)$ (Curtis 2020).

Figs. 2 and 3 clearly show the detected maneuvers, their timing, and the magnitude of the maneuvers' impulses. And the last figure shows that the TIANHUI-1 satellite in 2011 obtained mostly tangential impulses.

And finally, when we have the values of the tangential and binormal components of the impulses, we have evaluated the satellite impulse as $\Delta v_k=(\Delta v_{ktan}^2+\Delta v_{kbin}^2)^{1/2}$. The results are shown in Fig. 4.

Looking more closely at these figures, one can notice that often the maneuvers consist of several impulses. Accordingly, in order to determine the total impulse of each maneuver, it is necessary to sum up the values of the individual impulses of this group. This is shown in Table 1.

Table 1 Numerical results of detection and analysis of maneuvers of the TIANHUI-1 satellite

Maneuver	TLE epoch			Δa_k	Δv_{ktan}	Δi_k	Δv_{kbin}	Δv_k	Δv
#	Days of 2011	Date	Time	(m)	(m/s)	(deg)	(m/s)	(m/s)	(m/s)
1	31.889292	2011/01/31	21:20:35	17.161	0.010			0.010	0.010
2	33.002732	2011/02/02	00:03:56	-45.206	-0.025			0.025	0.025
3*	109.712863	2011/04/19	17:06:31	1496.148	0.830			0.830	0.854
	110.426439	2011/04/20	10:14:04	-42.637	-0.024			0.024	
4*	138.558854	2011/05/18	13:24:45	498.542	0.276	0.0016	0.211	0.347	0.377
	139.064758	2011/05/19	01:33:15	-24.035	-0.013			0.013	
	139.262223	2011/05/19	06:17:36	-30.954	-0.017			0.017	
5*	174.529292	2011/06/23	12:42:11	558.287	0.310			0.310	0.948
	174.781258	2011/06/23	18:45:01			-0.0029	-0.385	0.385	
	174.938035	2011/06/23	22:30:46			0.0017	0.226	0.226	
	175.128083	2011/06/24	03:04:26	-32.908	-0.018			0.018	
	175.527650	2011/06/24	12:39:49	-16.144	-0.009			0.009	
6*	210.011532	2011/07/29	00:16:36	204.638	0.114	0.0018	0.245	0.270	0.670
	210.597371	2011/07/29	14:20:13			-0.0017	-0.226	0.226	
	210.804548	2011/07/29	19:18:33			0.0011	0.146	0.146	
	212.508505	2011/07/31	12:12:15	-50.924	-0.028			0.028	
7*	237.732282	2011/08/25	17:34:29	295.827	0.164			0.164	0.239
	237.867241	2011/08/25	20:48:50	56.970	0.032			0.032	
	238.238304	2011/08/26	05:43:10	-77.968	-0.043			0.043	
8*	263.405595	2011/09/20	09:44:03	687.934	0.382			0.382	0.984
	263.743303	2011/09/20	17:50:21	-59.133	-0.033			0.033	
	263.937037	2011/09/20	22:29:20	-461.199	-0.256			0.256	
	264.065726	2011/09/21	01:34:39	510.512	0.283			0.283	
	264.388342	2011/09/21	09:19:13	-53.212	-0.030			0.030	
9	271.546446	2011/09/28	13:06:53	-17.072	-0.009			0.009	0.009
10	274.846006	2011/10/01	20:18:15	-20.544	-0.011			0.011	0.011
11*	282.919241	2011/10/09	22:03:42	598.013	0.331			0.331	0.350
	283.844624	2011/10/10	20:16:16	-34.663	-0.019			0.019	
12	296.505660	2011/10/23	12:08:09	-15.744	-0.009			0.009	0.009
13	298.821754	2011/10/25	19:43:20	-15.116	-0.008			0.008	0.017
	299.540465	2011/10/26	12:58:16	-16.772	-0.009			0.009	
14*	301.235208	2011/10/28	05:38:42	-19.197	-0.011			0.011	0.657
	301.908150	2011/10/28	21:47:44	983.292	0.545			0.545	
	302.226604	2011/10/29	05:26:19	-181.833	-0.101			0.101	
15	308.935599	2011/11/04	22:27:16	-30.673	-0.017			0.017	0.070
	309.856410	2011/11/05	20:33:14	-30.943	-0.017			0.017	
	310.907733	2011/11/06	21:47:08	-34.553	-0.019			0.019	
	311.893145	2011/11/07	21:26:08	-30.307	-0.017			0.017	
16	319.233275	2011/11/15	05:35:55	-20.413	-0.011			0.011	0.020
	320.547387	2011/11/16	13:08:14	-16.944	-0.009			0.009	
17*	321.652593	2011/11/17	15:39:44	1074.656	0.594	0.0029	0.385	0.708	1.108
	321.810757	2011/11/17	19:27:29	44.382	0.025	-0.0019	-0.252	0.254	
	321.940634	2011/11/17	22:34:31	20.113	0.011			0.011	
	322.130889	2011/11/18	03:08:29	-72.113	-0.040			0.040	
	322.925889	2011/11/18	22:13:17	54.673	0.030			0.030	
	323.181004	2011/11/19	04:20:39	-116.483	-0.065			0.065	

Table 1 Continued

18	325.539449	2011/11/21	12:56:48	-18.807	-0.010			0.010	0.010
19*	339.543118	2011/12/05	13:02:05	766.794	0.426			0.426	0.635
	339.803802	2011/12/05	19:17:28			-0.0015	-0.200	0.200	
	341.513468	2011/12/07	12:19:24	-16.054	-0.009			0.009	
20*	361.676711	2011/12/27	16:14:28	711.306	0.394	0.0052	0.687	0.792	2.510
	361.878404	2011/12/27	21:04:54	355.436	0.197	-0.0083	-1.101	1.118	
	362.068075	2011/12/28	01:38:02	87.016	0.048			0.048	
	362.261767	2011/12/28	06:16:57	-446.220	-0.248	0.0037	0.493	0.552	

Table 2 Number of the detected TIANHUI-1 satellite maneuvers and their distribution

Number of the detected maneuvers	Distribution according to the magnitude of the impulse		Distribution according to the types of impulses (according to the types of maneuvers)		
	Δv<0.06 м/с	Δv>0.06 м/с	tangential (in-plane maneuvers)	combined	binormal (out-of-plane maneuvers)
20	9	11	14	6	0

Detailed numerical results of detection and analysis of maneuvers are given in Table 1. The table shows the results of calculations of changes in the semi-major axis (Δa_k) and inclination (Δi_k), tangential (Δv_{ktan}) and binormal (Δv_{kbin}) components of the impulse, as well as the value of the impulse (Δv_k). The first column of the table gives the maneuver numbers, and the last column gives the total impulses of the maneuvers. TLEs epochs are given as days of 2011, date and UTC time. It should be noted that these epochs do not reflect the exact moments of the maneuvers. They are TLE epochs on which maneuvers were found. In fact, the maneuvers were carried out between the current and previous TLE moments. Since the maneuver is detected based on the difference in the semi-major axis and inclination between the current and previous TLEs, the frequent determination of the TLEs during the day can smooth out this difference, and in certain cases the maneuver may not be detected. This must be taken into account when detecting a maneuver and determining the total impulse of the maneuver.

Analyzing the data in Table 1, we found 20 maneuvers. Impulses of $\Delta v \geq 0.01$ m/s are taken as detected maneuvers. For qualitative analysis, we divided all maneuvers into two groups: small maneuvers with impulses of Δv<0.06 m/s, and relatively large maneuvers with impulses of Δv>0.06 m/s. The latter in Table 1 are indicated by an asterisk (*).

As can be seen from this table, some maneuvers were carried out within 2-3 days. We combined them into one maneuver. Each such maneuver was either tangential or combined with a binormal maneuver.

Table 2 shows the number of detected maneuvers, their distribution according to the magnitude of the impulse and according to the types of impulses (tangential and binormal), and, according to the types of maneuvers (in-plane and out-of-plane).

Of the 20 maneuvers we found, 11 are relatively strong maneuvers and they stand out in Fig. 4. Moreover, 14 maneuvers are in-plane maneuvers and 6 are combined ones. Thus, it can be argued that this satellite in 2011 was controlled mainly on the semi-major axis. Bai *et al*. (2019) also studied the TIANHUI-1 satellite in 2011 and they found a total of 11 maneuvers. These are the 11 maneuvers we found. But our method made it possible to detect an additional 9 weaker maneuvers.

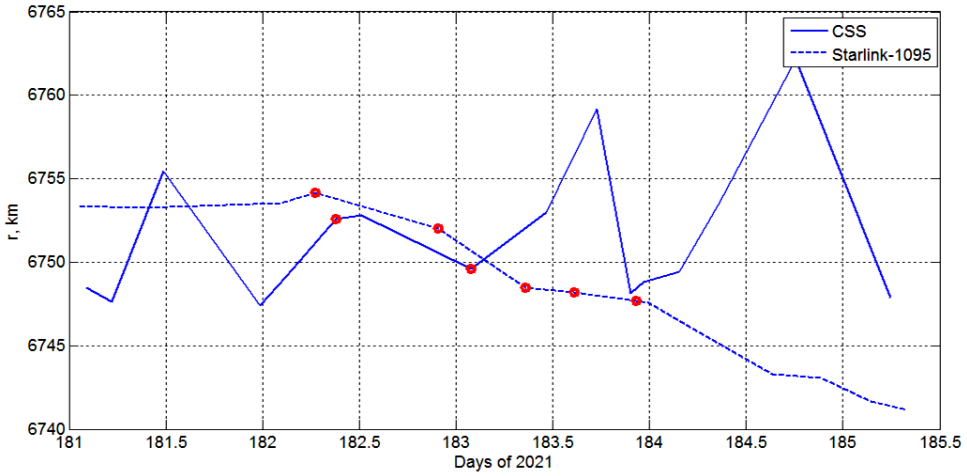

Fig. 5 Geocentric distances of the CSS and the Starlink-1095 satellite from June 30 (day 181) to July 4 (day 185), 2021

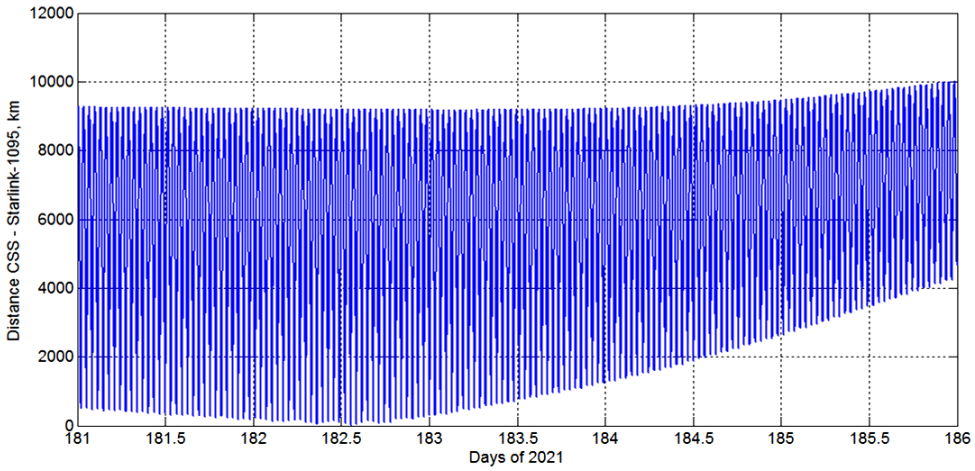

Fig. 6 Variation in the relative distances between CSS and the Starlink-1095 satellite

Summarizing, it can be argued that the proposed method made it possible to obtain a complete picture of the TIANHUI-1 satellite maneuvers.

3.2 China space station, Starlink-1095 and Starlink-2305

After test-applying the proposed method to the TIANHUI-1 satellite, and proving the applicability of this method to the detection and analysis of performed maneuvers, we applied this method to the analysis of the maneuvers of the China Space Station - TIANHE-1 (NORAD ID 48274), Starlink-1095 (NORAD ID 44971) and Starlink-2305 (NORAD ID 47989).

3.2.1 Case 1 July 2021

As noted in Section 1, a close encounter occurred between the Starlink-1095 satellite and the

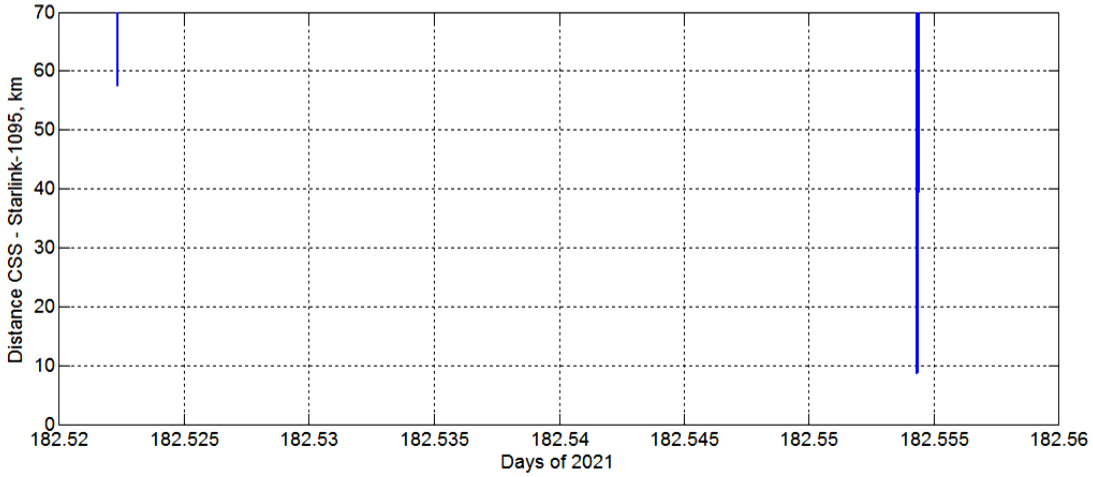

Fig. 7 Minimum distances at closest approach of CSS and the Starlink-1095

China Space Station on 1 July 2021 and the China Space Station (CSS) performed an evasive maneuver to avoid a potential collision between the two spacecraft. We investigated this case from the point of view of detection and analysis of maneuvers carried out by satellites. For this purpose, historical TLEs data of these satellites for 2021 were downloaded from the CelesTrak website (2022). Before applying our method to this case, we determined the geocentric distances of the CSS and the Starlink-1095 satellite from June 30 (day 181) to July 4 (day 185) of that year to find out their relative position in height. The satellite coordinates are obtained from TLE elements using the SGP4 model. The results are shown in Fig. 5. The red circles show the moments of TLE for which the maneuvers are detected.

In addition, in order to demonstrate the necessity for orbital maneuvers, we analyzed the variation in the relative distances between the CSS and Starlink-1095 over the specified period. The results are presented in Fig. 6. Here we observe a periodic change in these distances during the day. We also observe how the minimum distance decreases until July 1, and how this distance began to increase after the necessary maneuvers were performed.

To assess the degree of collision threat, we have identified a time interval corresponding to the minimum distances. The results are shown in Fig. 7.

As we can see from this figure, the minimum distance was approximately 57 km on July 1, 12:31 (UTC). The next dangerous approach happened at 13:17 (UTC), i.e. 46 minutes after the first approach, and this time, these two spacecraft approached at a distance of about 9 km. But the actual distance may have been less than we predicted.

To detect and analyze the maneuvers of the CSS, we processed its TLE data for the period from June 30 (day 181) to July 4 (day 185), 2021 using our algorithm described in Section 2. As a result, we found the maneuvers carried out during this time. The impulses of these maneuvers are shown in Fig. 8. Here we do not present graphs of intermediate results, as was done in the case of the TIANHUI-1 satellite. There it was done to demonstrate in detail the essence of the algorithm and its capabilities.

On Fig. 8 all maneuvers performed during the period under review are clearly visible. And detailed numerical results of detection and analysis of maneuvers are given in Table 3.

In this table, the TLE epochs are given in days of the year, date and UTC time. The following

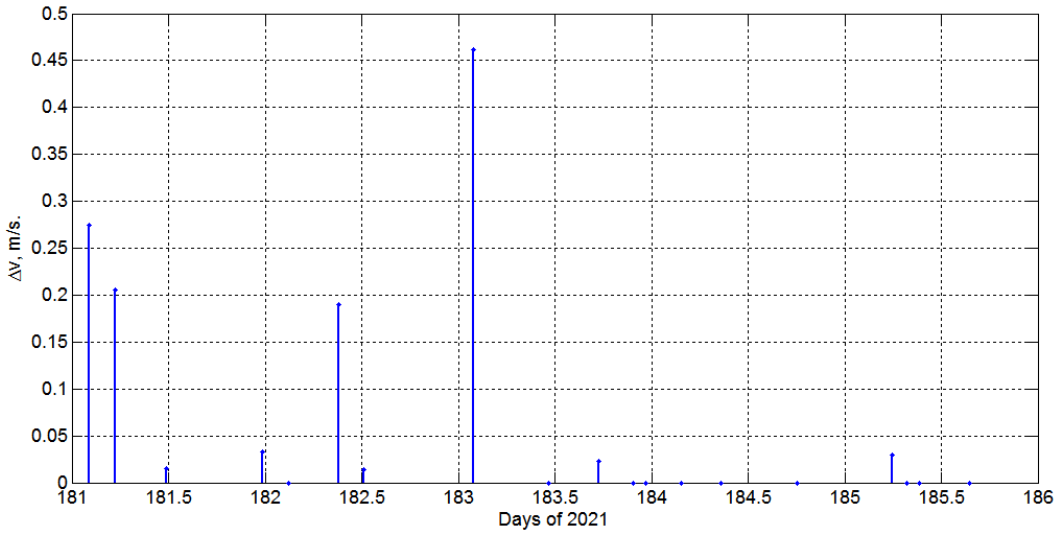

Fig. 8 Detected CSS maneuvers for the period from June 30 (day 181) to July 4 (day 185), 2021 and the magnitude of their impulses

Table 3 Numerical results of detection and analysis of maneuvers of the CSS for the period from June 30 (day 181) to July 4 (day 185), 2021

TLE epoch of CSS			Δa_k	Δv_{ktan}	Δi_k	Δv_{kbin}	Δv_k
Days of 2021	Date	Time	(m)	(m/s)	(deg)	(m/s)	(m/s)
181.087441	**2021/06/30**	**02:05:55**	**-481.89**	**-0.274**			**0.274**
181.222393	**2021/06/30**	**05:20:15**	**74.93**	**0.043**	**0.002**	**0.201**	**0.206**
181.489088	2021/06/30	11:44:17	-26.78	-0.015			0.015
181.987983	2021/06/30	23:42:42	-58.40	-0.033			0.033
182.379899	**2021/07/01**	**09:07:03**			**-0.001**	**-0.189**	**0.189**
182.509170	2021/07/01	12:13:12	-24.85	-0.014			0.014
183.078613	**2021/07/02**	**01:53:12**	**810.63**	**0.461**			**0.461**
183.728101	2021/07/02	17:28:28	39.23	0.022			0.022
185.246320	2021/07/04	05:54:42	52.38	0.030			0.030

columns show changes in the semi-major axis (Δa_k), tangential components of the impulse (Δv_{ktan}), changes in the inclination (Δi_k), binormal components of the impulse (Δv_{kbin}), and the value of the impulse (Δv_k).

As follows from this Table, 9 maneuvers were performed during the period under review. Of these, four maneuvers are significant: two maneuvers performed on 30 June (days 181.087441 and 181.222393), the out-of-plane maneuvers carried out on 1 July (day 182.379899) and the in-plane maneuver carried out on 2 July (day 183.078613). The data of these maneuvers in the table are highlighted in bold. It should be noted here that the indicated days and times are the TLE epochs on which these maneuvers were detected. So the maneuvers could have been carried out earlier, for example, not on 2 July, but on 1 July.

As noted in the China Note (United Nations 2021), a close encounter occurred between the Starlink-1095 satellite and the China Space Station on 1 July 2021 and the CSS took the initiative

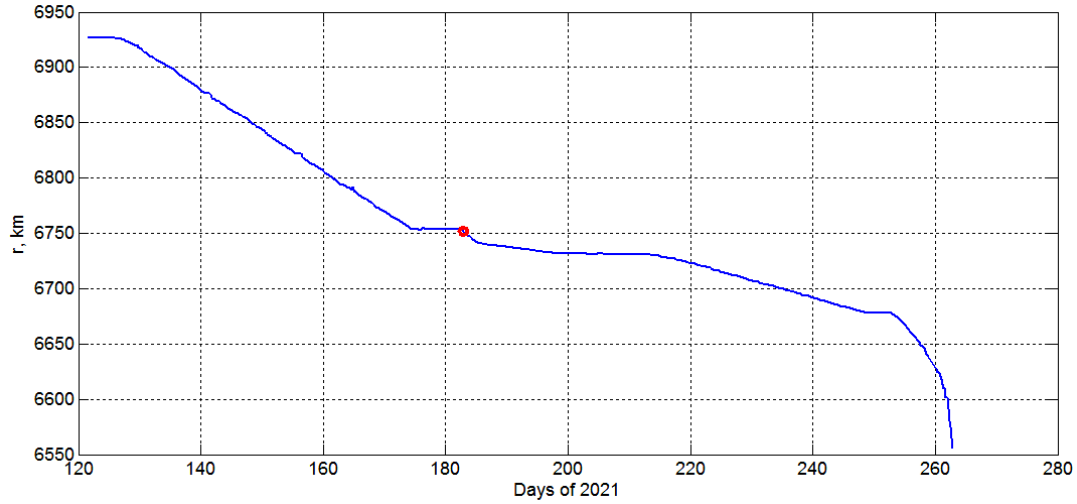

Fig. 9 Geocentric distances of the Starlink-1095 satellite from May 1 (day 121) to September 19 (day 262), 2021

to conduct an evasive maneuver in the evening of that day. So, we are primarily interested in the maneuvers carried out on July 1 and 2. We found that as a result of these maneuvers, the orbital inclination decreased by 0.001 degrees and the semi-major axis increased by 810.63 m. The corresponding impulses were 0.189 m/s and 0.461 m/s.

The two maneuvers noted above, which were performed on 30 June, were in-plane maneuver and combined one respectively. As a result of the first maneuver, the semi-major axis has been reduced by 481.89 m. And as a result of the second maneuver, the semi-major axis has been increased by 74.93 m, but most importantly, the inclination has been increased by 0.002 degrees, which corresponds to a linear deviation of the CSS by about 236 m. The CSS from 30 June to 4 July increased its semi-major axis by a total of 385 m.

Now, against the background of this event, it would be interesting to consider the maneuvers of the Starlink-1095 satellite. As noted in the China Note (United Nations, 2021), as from 19 April 2020, the Starlink-1095 satellite had been travelling stably in orbit at an average altitude of around 555 km. Between 16 May and 24 June 2021, the Starlink-1095 satellite maneuvered continuously to an orbit of around 382 km, and then stayed in that orbit. Therefore, we processed Starlink-1095 satellite TLE data for the period from May 1 (day 121) to September 19 (day 262), 2021. Fig. 9 shows the changes in its geocentric distance during this period. The red circle marks 1 July (day 182). This plot shows that the Starlink-1095 satellite systematically lowered its altitude during the period under review. But from June 24 to July 1, it stopped the decrease in height. After that, it continued to reduce the height until complete deorbited.

Fig. 10 shows tangential and binormal components of the Starlink-1095 satellite maneuver impulses for the period from May 1 to September 19, 2021. Both Figs. 9 and 10 give reason to believe that in the interval from June 24 to July 1 the Starlink-1095 satellite had not carried out significant maneuvers. They started July 1st (day 182).

It is noteworthy that almost all maneuvers were in-plane maneuvers and reduced the semi-major axis. As a result, the geocentric distance was constantly decreasing, i.e., the height kept decreasing.

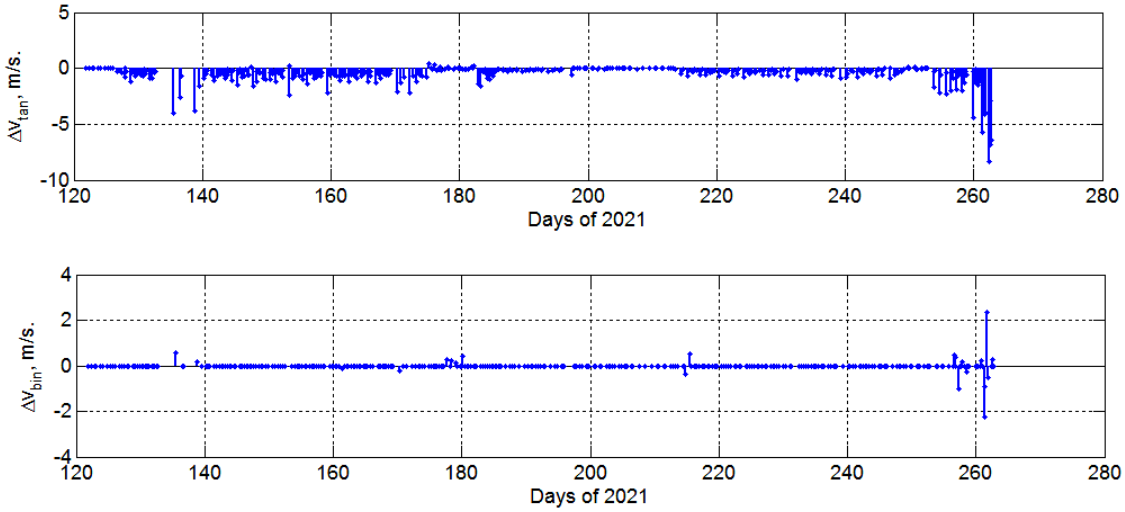

Fig. 10 Tangential and binormal components of the Starlink-1095 satellite maneuver impulses for the period from May 1 to September 19, 2021

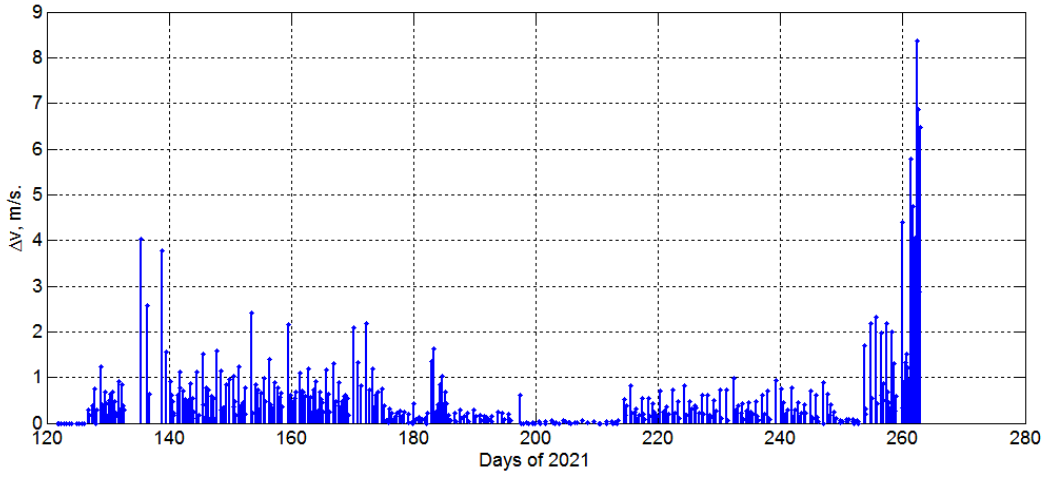

Fig. 11 Maneuver impulses of the Starlink-1095 satellite for the period from May 1 to September 19, 2021

Fig. 11 is interesting from the point of view of the maneuvering process energy. It presents the results of evaluating the impulses of the maneuvers. Satellite impulses of the maneuvers evaluated from the tangential and binormal components as $\Delta v_k=(\Delta v_{ktan}{}^2+\Delta v_{kbin}{}^2)^{1/2}$. The figure gives information about the intensity of maneuvers, i.e., about the frequency of maneuvers and the magnitude of impulses.

As can be seen from the diagram, the intensity of the maneuvers of the Starlink-1095 satellite in July (days 182-212) decreased. Although during the days of its approach to the CSS from July 1 to 4, quite strong maneuvers were performed. On August 1 (day 213) the maneuvers resumed. And from September 10 (day 253) more intensive maneuvers began and the last maneuver was on September 19 (day 262). On 20 September 2021 the satellite was deorbited.

Table 4 Numerical results of detection and analysis of the Starlink-1095 maneuvers for the period from June 30 (day 181) to July 3 (day 184), 2021

TLE epoch of Starlink-1095			Δa_k	Δv_{ktan}	Δi_k	Δv_{kbin}	Δv_k
Days of 2021	Date	Time	(m)	(m/s)	(deg)	(m/s)	(m/s)
181.057990	2021/06/30	01:23:30	-84.11	-0.048			0.048
181.377380	2021/06/30	09:03:26	-145.92	-0.083			0.083
181.952306	2021/06/30	22:51:19	201.70	0.115			0.115
182.271732	**2021/07/01**	**06:31:18**	**405.63**	**0.231**			**0.231**
182.910437	**2021/07/01**	**21:51:02**	**-2 367.58**	**-1.347**			**1.347**
183.357192	**2021/07/02**	**08:34:21**	**-2 845.44**	**-1.62**			**1.62**
183.612420	**2021/07/02**	**14:41:53**	**-440.08**	**-0.25**			**0.25**
183.931417	**2021/07/02**	**22:21:14**	**-690.81**	**-0.393**			**0.393**
183.995211	2021/07/02	23:53:06	-120.50	-0.069			0.069
184.250330	2021/07/03	06:00:29	-1 495.60	-0.852			0.852
184.632841	2021/07/03	15:11:18	-1 800.49	-1.026			1.026
184.887788	2021/07/03	21:18:25	-717.91	-0.409			0.409

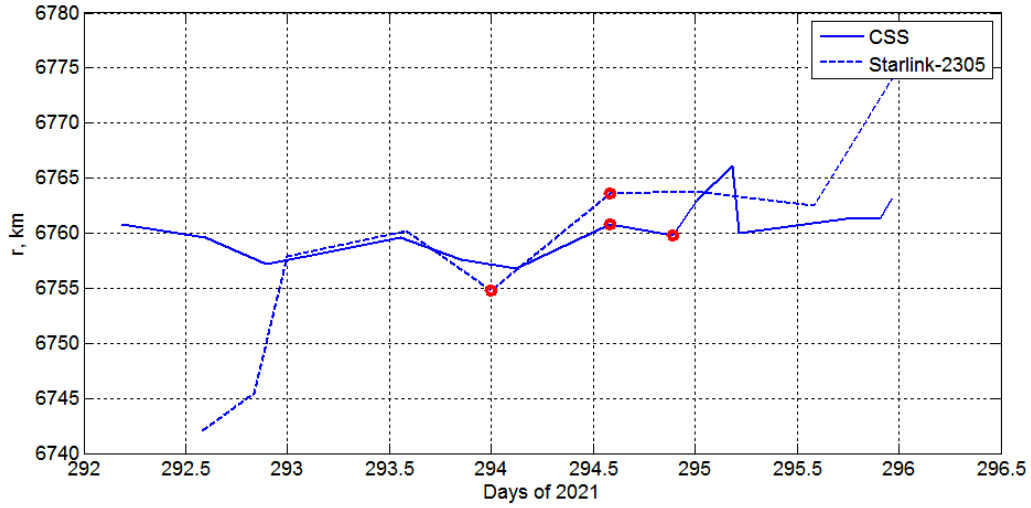

Fig. 12 Geocentric distances of the CSS and the Starlink-2305 satellite from October 19 (day 292) to October 22 (day 295), 2021

Table 4 shows the detailed numerical results of detection and analysis of the Starlink-1095 maneuvers in the vicinity of the days of the incident, i.e., from June 30 (day 181) to July 3 (day 184), 2021.

As can be seen from this table, the Starlink-1095 satellite conducted active maneuvers on July 1 and 2. These data are highlighted in bold. Except for one maneuver, all maneuvers reduced the semi-major axis, i.e., these maneuvers were aimed at lowering the orbit. Fig. 5 confirms this. All maneuvers were only in-plane. There was no change in the orbital inclination during this period.

From May 1 to September 19, the semi-major axis of the Starlink-1095 satellite decreased by 358.596 km as a result of maneuvers, including from June 30 to July 3 by 10.101 km.

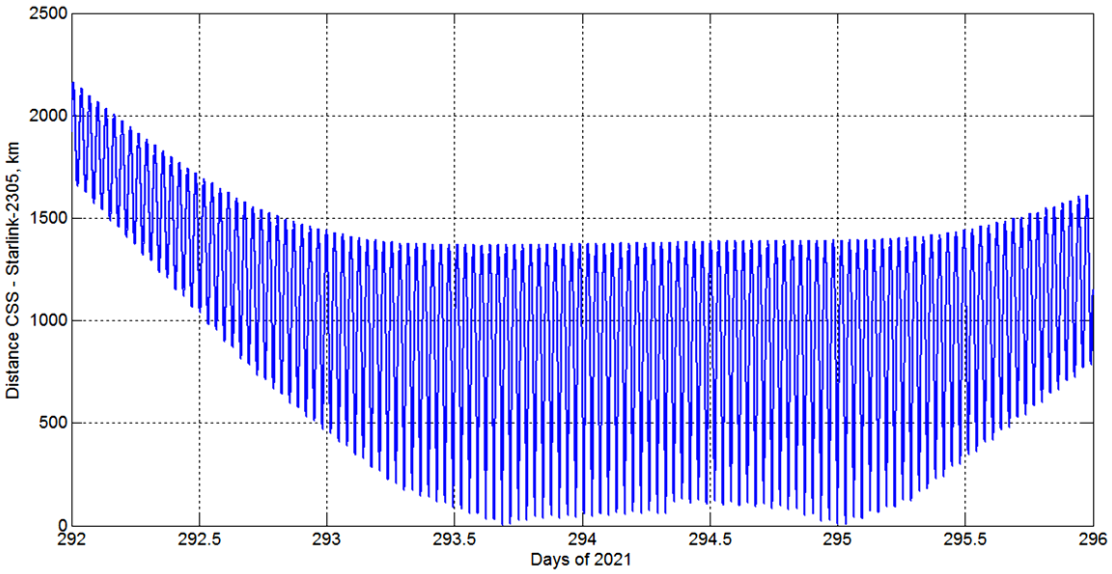

Fig. 13 Variation in the relative distances between CSS and the Starlink-2305 satellite from October 19 (day 292) to October 22 (day 295), 2021

3.2.2 Case 21 October 2021

As noted in document (United Nations, 2021), the second incident occurred on October 21, 2021, when the Starlink-2305 satellite had a subsequent close encounter with the CSS. As the satellite was continuously maneuvering, the maneuver strategy was unknown and orbital errors were hard to be assessed, there was thus a collision risk between the Starlink-2305 satellite and the CSS. To ensure the safety and lives of in-orbit astronauts, the CSS performed an evasive maneuver again on the same day to avoid a potential collision between the two spacecraft.

To analyze this event, we downloaded historical TLE data of the Starlink-2305 satellite for the period from September 1 (day 244) to December 30 (day 364) 2021 from the CelesTrak website (2022). Based on the TLE data, the geocentric distances of these satellites were determined. Fig. 12 shows the changes in the geocentric distances of these satellites from October 19 (day 292) to October 22 (day 295), 2021. Red circles indicate maneuvers on October 21, 2021.

As in the case of Starlink-1095, in order to demonstrate the necessity for orbital maneuvers, we analyzed the variation in the relative distances between the CSS and Starlink-2305 over the specified period. The results are presented in Fig. 13. Here we observe a periodic change in these distances during the day and close approaches between days from 292.5 to 295.2. In addition, this figure shows a confident increase in the relative distance after the maneuvers performed.

To assess the degree of collision threat, we have identified a time intervals corresponding to the minimum distances. The results are shown in Figs. 14 and 15.

As we can see from this figures, the minimum distance was 4 times: approximately 4 km on October 20, 16:31 (UTC), 6 km on October 20, 17:16 (UTC), 8.5 km on October 22, 00:01 (UTC) and 7.5 km on October 22, 00:46 (UTC). But the actual distance may have been less than we predicted.

Having processed the CSS TLE data for the period from October 19 (day 292) to October 22 (day 295) according to our algorithm, we detected the maneuvers and estimated the magnitudes of

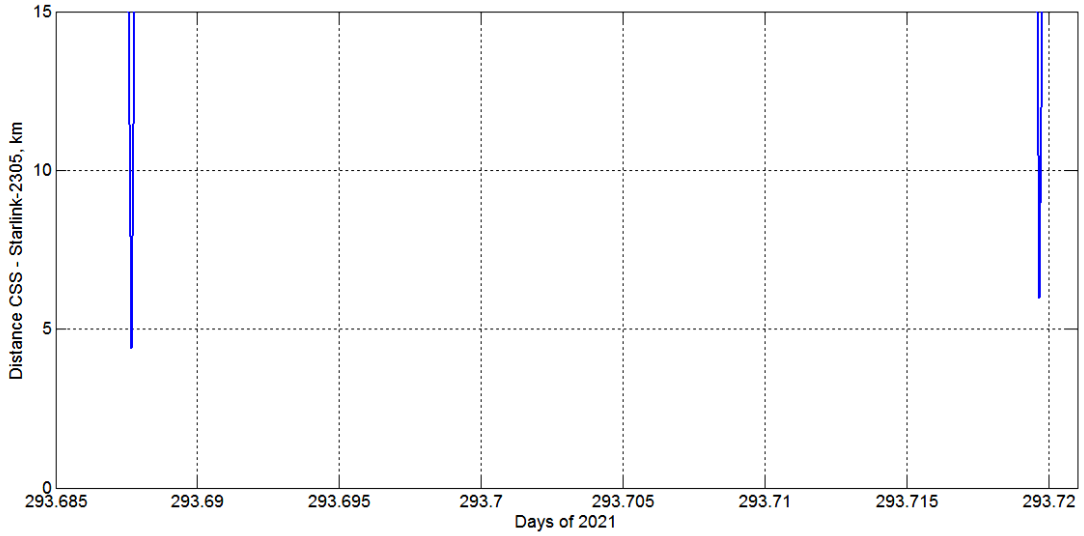

Fig. 14 Minimum distances at closest approach of CSS and the Starlink-2305 October 20, 2021

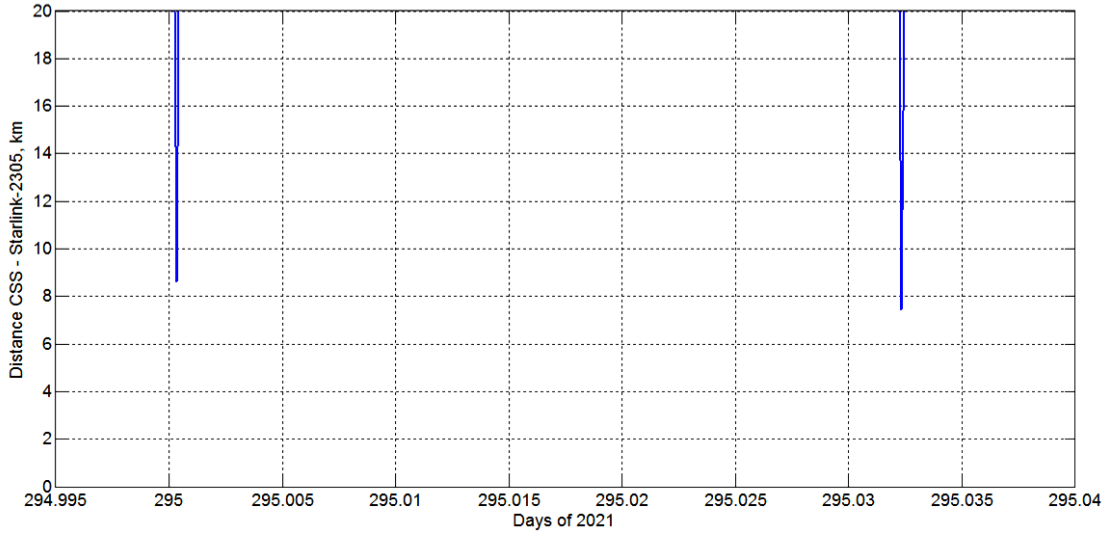

Fig. 15 Minimum distances at closest approach of CSS and the Starlink-2305 October 22, 2021.

their impulses. The results are shown in Fig. 16.

All maneuvers are clearly distinguished here, and especially the maneuvers of October 21 (day 294). One tangible CSS maneuver is visible here, performed on October 19 (day 292), i.e., two days before the incident. It will be shown below that this maneuver was a maneuver for changing the inclination of the CSS orbit.

And detailed numerical results of detection and analysis of maneuvers are given in Table 5.

As follows from the Table 5, 10 maneuvers were performed during the period under review. Of these, three maneuvers are significant. The data of these maneuvers in the table are highlighted in bold. All three maneuvers are combined maneuvers. The main maneuver that saved the CSS from

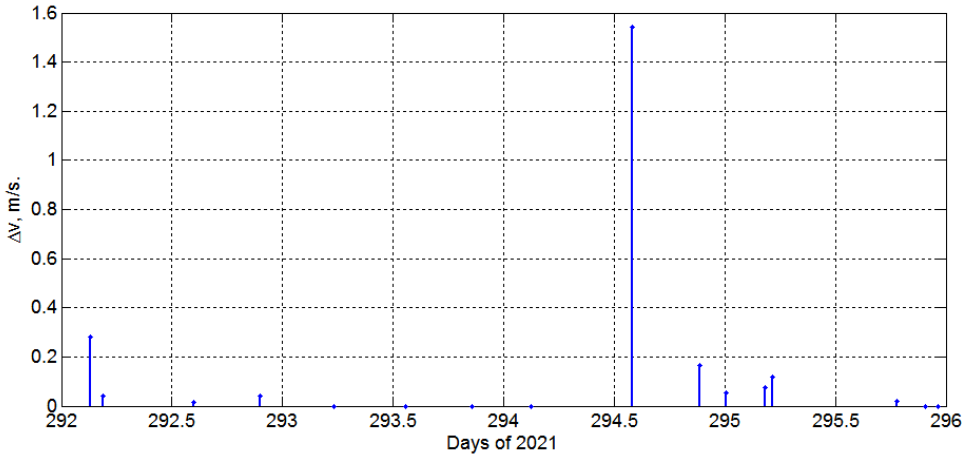

Fig. 16 Detected CSS maneuvers for the period from October 19 (day 292) to October 22 (day 295), 2021 and the magnitude of their impulses

Table 5 Numerical results of detection and analysis of maneuvers of the CSS for the period from October 19 (day 292) to October 22 (day 295), 2021

TLE epoch of CSS			Δa_k	Δv_{ktan}	Δi_k	Δv_{kbin}	Δv_k
Days of 2021	Date	Time	(m)	(m/s)	(deg)	(m/s)	(m/s)
292.131934	**2021/10/19**	**03:09:59**	**-21.25**	**-0.012**	**0.002**	**0.280**	**0.281**
292.186097	2021/10/19	04:27:59	-68.60	-0.039			0.039
292.597124	2021/10/19	14:19:52	28.62	0.016			0.016
292.896671	2021/10/19	21:31:12	-68.13	-0.039			0.039
294.580338	**2021/10/21**	**13:55:41**	**2 537.45**	**1.440**	**-0.004**	**-0.555**	**1.543**
294.888653	**2021/10/21**	**21:19:40**	**60.54**	**0.034**	**0.001**	**0.162**	**0.166**
295.007514	2021/10/22	00:10:49	-95.43	-0.054			0.054
295.183917	2021/10/22	04:24:50	136.04	0.077			0.077
295.215646	2021/10/22	05:10:32	-205.46	-0.117			0.117
295.780341	2021/10/22	18:43:41	36.72	0.021			0.021

a possible collision with the Starlink-2305 satellite is the maneuver on October 21 (day 294.580338). This maneuver increased the semi-major axis by 2537.45 m and decreased the orbital inclination by 0.004 degrees, which corresponds to a linear deviation of about 470 m. The impulse of this maneuver was 1.543 m/s. The rest of the maneuvers had no significant effect on the orbital elements. The CSS in the period from October 19 to 22 increased its semi-major axis by a total of 2341 m.

Now consider the movement of the Starlink-2305 satellite and its maneuvers. For this purpose, we processed his TLE data for the period from September 1 (day 244) to December 30 (day 364), 2021. We began our study by determining the geocentric distance of this satellite. Fig. 17 shows the changes in its geocentric distance during this period. The red circle marks October 21 (day 294). As can be seen from this figure, starting from October 16 (day 289), the geocentric distance (and, accordingly, the height) began to increase. This increase continued until approximately November 18 (day 322). And from October 19 to 22, close encounters of this satellite with the

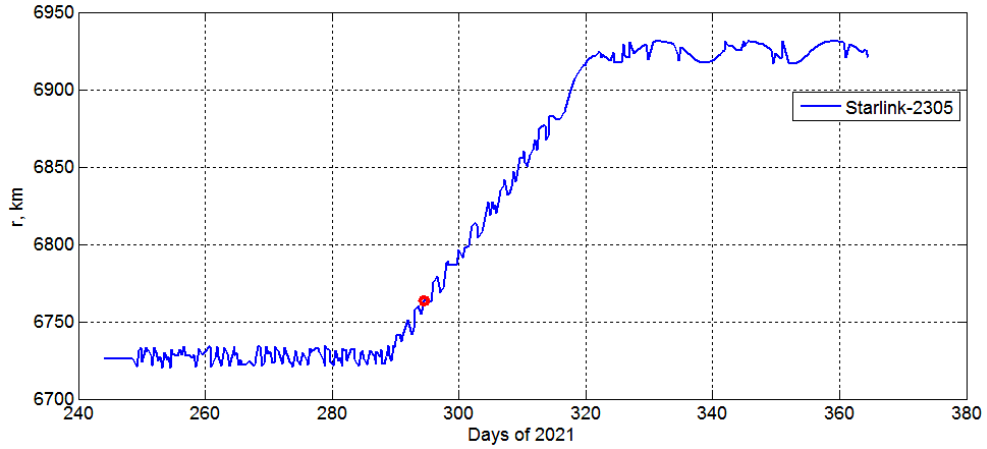

Fig. 17 Geocentric distances of the Starlink-2305 satellite from September 1 (day 244) to December 30 (day 364), 2021

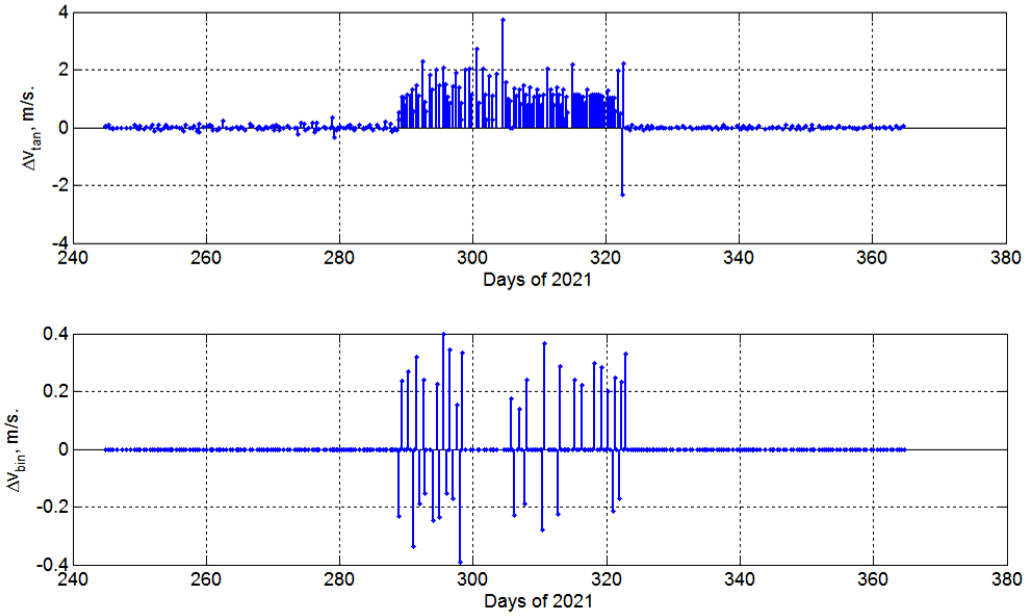

Fig. 18 Tangential and binormal components of the Starlink-2305 satellite maneuver impulses for the period from September 1 (day 244) to December 30 (day 364), 2021

CSS occurred. The fluctuation character of the change in the distance in Fig. 17 is explained by the fact that we built this graph using the values obtained only for the TLE epochs. In fact, these distances change periodically during the day. Since the number of such epochs during the day is only a few, and they are not periodic, the distance graph is obtained as if with noise.

Using our algorithm, we detected the maneuvers of this satellite and calculated their impulses. Fig. 18 shows tangential and binormal components of the Starlink-2305 satellite maneuver impulses for the period from September 1 (day 244) to December 30 (day 364), 2021.

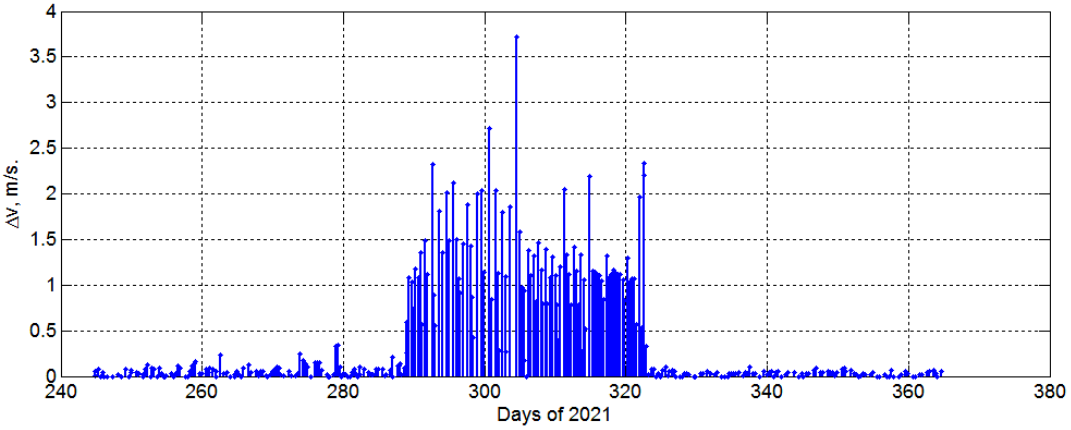

Fig. 19 Maneuver impulses of the Starlink-2305 satellite for the period from September 1 (day 244) to December 30 (day 364), 2021

Table 6 Numerical results of detection and analysis of the Starlink-2305 maneuvers for the period from October 19 (day 292) to October 22 (day 295), 2021

TLE epoch of Starlink-2305			Δa_k	Δv_{ktan}	Δi_k	Δv_{kbin}	Δv_k
Days of 2021	Date	Time	(m)	(m/s)	(deg)	(m/s)	(m/s)
292.583345	2021/10/19	14:00:01	4 045.03	2.306	0.002	0.24	2.319
292.833345	2021/10/19	20:00:01	1 531.41	0.872	-0.001	-0.153	0.886
293.000012	2021/10/20	00:00:01	973.63	0.554			0.554
293.583345	2021/10/20	14:00:01	3 179.65	1.806			1.806
294.000012	**2021/10/21**	**00:00:01**	**2 338.47**	**1.329**	**-0.002**	**-0.246**	**1.352**
294.583345	**2021/10/21**	**14:00:01**	**3 523.62**	**1.999**	**0.002**	**0.227**	**2.012**
295.000023	2021/10/22	00:00:02	2 580.84	1.464	-0.002	-0.237	1.483
295.583345	2021/10/22	14:00:01	3 664.58	2.079	0.003	0.397	2.117

The results of the analysis show that active maneuvers were carried out from October 16 (day 289) to November 18 (day 322) 2021. Most of the maneuvers are in-plane maneuvers that have increased the semi-major axis. Thus, the height of the satellite during this period was constantly increasing. This is confirmed by Fig. 17. Out-of-plane maneuvers were carried out from October 16 (day 289) to October 25 (day 298) and from November 1 (day 305) to November 18 (day 322).

The values of the total impulse of each maneuver are determined from the tangential and binormal components of the maneuver impulses. The results are presented in Fig. 19. This figure also confirms that the main maneuvers were carried out from October 16 to November 18, 2021.

Now, from the general picture of the maneuvers of the Starlink-2305 satellite, we select those that were in the vicinity of the day of the incident, i.e., October 21. Table 6 shows the detailed numerical results of detection and analysis of the Starlink-2305 maneuvers from October 19 (day 292) to October 22 (day 295), 2021.

As can be seen from this Table, 8 maneuvers were performed during the indicated three days. On the day of the incident, when the CSS performed evasive maneuvers on October 21, Starlink-2305 also conducted maneuvers. They are highlighted in bold. It should be noted that all the maneuvers of these days were with a large increase in the semi-major axis, and most of them were

combined with maneuvers to change the inclination of the orbit.

And finally, it should be noted that from September 1 to December 30, the total increase in the semi-major axis of the Starlink-2305 satellite was 195.917 km, including from October 19 to October 22 by 21.837 km.

4. Conclusions

The proposed method is considered as a solution to one of the important tasks of space surveillance and space situation awareness. This is the task of detecting satellite maneuvers and analyzing their impulses. It is important not only to detect satellite maneuvers, but also to analyze them, evaluate their consequences, and determine changes in orbital parameters. The analysis of the maneuvers will make it possible to estimate the fuel consumption for the maneuver. Although the principle of detecting maneuvers based on historical TLE data and jumps of the semi-major axis and inclination is not new, we introduced some improvements. First, we use the difference of two osculating elements, which are both obtained by propagation using the SGP4 model (for LEO satellites), as an indicator of maneuver detection. Secondly, our method allows not only to detect maneuvers, but also to get a more complete picture of the maneuver. In particular, the method makes it possible to estimate the moments of the beginning and end of the maneuver, calculate the changes in the orbital elements, evaluate the tangential and binormal components of the impulse, and finally, calculate the impulse of the satellite obtained as a result of the maneuver.

Although we have applied our method to LEO satellites, it can be applied to other types of satellites, e.g., to geostationary satellites. But in this case it will be necessary to use the SDP4 model. In addition, in our calculations we assumed that the orbits have negligible eccentricities. If the method is applied to orbits that do not satisfy these conditions, then this will have to be taken into account in the formulas for calculating tangential and binormal impulse components. In the future, we plan to test this method on the operating GEO satellites, as well as introduce some improvements to it.

It may be stated that the proposed method can be used to monitor maneuvers or other anomalous changes in the orbit of a large number of satellites in near real time. In order to show the possibility of this method for monitoring, we estimated the complexity of this algorithm. For this purpose, the execution time for the TIANHUI-1 satellite for 2011 was estimated. Calculations were carried out on a computer with RAM 4 GB and 1.8 GHz processor speed, and processed historical TLE data for 1221 epochs. The computation time was 0.548 seconds, i.e., the average processing time for TLE data per epoch is approximately 0.449 msec. Time to read the TLE data, output the results to a file, and build Fig. 4 took an additional 1.049 seconds. Thus, the total time was 1.597 sec. These calculations show that the proposed algorithm can indeed process the current TLE data for a large number of satellites almost in near real time. For example, for 1000 satellites, the TLE data processing time for the two epochs is approximately 1 sec. All this shows that on the basis of this algorithm it is possible to create a service for monitoring satellite maneuvers.

References

Bai, X., Liao, C., Pan, X. and Xu, M. (2019), "Mining two-line element data to detect orbital maneuver for satellite", *IEEE Access*, **7**, 129537-129550. https://doi.org/10.1109/access.2019.2940248.

CelesTrak (2022), NORAD Two-Line Element Sets. https://celestrak.com/NORAD/archives/request.php.
Chen, L., Bai, X.Z., Liang, Y.G. and Li, K.B. (2017), *Orbital Data Applications for Space Objects*, Springer, Singapore.
Clark, R. and Lee, R. (2020), "Parallel processing for orbital maneuver detection", *Adv. Space Res.*, **66**(2), 444-449. https://doi.org/10.1016/j.asr.2020.04.010 .
Curtis, H. (2020), *Orbital Mechanics for Engineering Students*, Elsevier, Butterworth-Heinemann, Oxford, UK.
ESA (2019), ESA Spacecraft Dodges Large Constellation, https://www.esa.int/Safety_Security/ESA_spacecraft_dodges_large_constellation.
Hoots, F.R. and Roehrich, R.L. (1980), *Spacetrack Report #3: Models for Propagation of the NORAD Element Sets*, U.S. Air Force Aerospace Defense Command, Colorado Springs, CO.
Hu, W. (2015), *Fundamental Spacecraft Dynamics and Control*, John Wiley & Sons Singapore Pte. Ltd., Singapore.
Kelecy, T., Hall, D., Hamada, K. and Stocker, D. (2007), "Satellite maneuver detection using two-line Element (TLE) data", *Proceedings of the Advanced Maui Optical and Space Surveillance Technologies Conference*, Hawaii, USA, September.
Lemmens, S. and Krag, H. (2014), "Two-line-elements-based maneuver detection methods for satellites in low Earth orbit", *J. Guidan. Control Dyn*., **37**(3), 860-868. https://doi.org/10.2514/1.61300.
Li, T., Li, K. and Chen, L. (2018), "New manoeuvre detection method based on historical orbital data for low Earth orbit satellites", *Adv. Space Res*., **62**(3), 554-567. https://doi.org/10.1016/j.asr.2018.05.002.
Li, T., Li, K. and Chen, L. (2019), "Maneuver detection method based on probability distribution fitting of the prediction error", *J. Spacecraft Rocket*., **56**(4), 1114-1120. https://doi.org/10.2514/1.A34301.
Liu, J., Liu, L., Du, J. and Sang, J. (2021), "TLE outlier detection based on expectation maximization algorithm", *Adv. Space Res*., **68**(7), 2695-2712. https://doi.org/10.1016/j.asr.2021.07.013.
Mukundan, A. and Wang, H.C. (2021), "Simplified approach to detect satellite maneuvers using TLE data and simplified perturbation model utilizing orbital element variation", *Appl. Sci*., **11**(21), 10181-10195. https://doi.org/10.3390/app112110181.
Patera, R.P. (2008), "Space event detection method", *J. Spacecraft Rocket*., **45**(3), 554-559. https://doi.org/10.2514/1.30348.
Spacenews (2019), ESA Spacecraft Dodges Potential Collision with Starlink Satellite, https://spacenews.com/esa-spacecraft-dodges-potential-collision-with-starlink-satellite/
United Nations (2021), Office for Outer Space Affairs, A/AC.105/1262. https://www.unoosa.org/oosa/en/oosadoc/data/documents/2021/aac.105/aac.1051262_0.html.

CC